WAS Science Nature
WASSN

ISSN: 2766 - 7715
WAS PRESS

Article

Deep Learning Model for Magnetic Resonance Imaging Brain Tumor Recognition

Abir Fettah[1], Bouchra Goumidi[1] and Mostafa El Habib Daho [1,*]

[1] Biomedical Engineering Laboratory, University of Tlemcen, Algeria;
* Correspondence: mostafa.elhabibdaho@univ-tlemcen.dz

Received: 07-02-2021; Accepted: 20-05-2021; Published: 01-01-2022

Abstract: Human interpretation of a large quantity of Magnetic Resonance Imaging (MRI images) is a tiring task and depends on the practitioner's expertise and experience. Glioma is one of the most common and dangerous types of primary brain tumors, and its early diagnosis could be life-saving. Precise and fully automatic classification of Glioma on MRI images helps physicians diagnose and monitor patients.
In this work, we propose an automatic system to aid in diagnosing Glioma by classifying brain tumors into two categories: High-Grade Glioma (HGG) and Low-Grade Glioma (LGG). To perform this task, we trained three deep learning models (VGG-16, ResNet-50, and Inception-V3) on four brain MRI datasets (one for each MRI modality). To further improve tumor classification, non-tumorous slices were removed from the HGG class of the selected dataset and then were separately used to train the three models. Evaluations on BraTS 2019 attest that T1 presents the most discriminative features with 0.9513, 0.907, and 0.9487 for accuracy, sensitivity, and specificity, respectively. The Inception-V3 model outperforms the other models with 0.9975, 0.9894, and 1 for accuracy, sensitivity, and specificity. Experimental results demonstrate that using the Inception-V3 model with T1 modality can achieve good performances.

Keywords: Glioma, MRI, Deep Learning, Brain Tumor classification, CNN, LGG, HGG.

1. Introduction

The brain is one of the foremost complex organs within the human body that works with billions of cells. Sometimes, these cells can be exposed to an uncontrolled cell division and formed an abnormal group of cells around or inside the brain; that's what we call brain tumors. This kind of tumor can affect the traditional functionality of brain activity and cause many problems.
Cerebral tumors are classed to benign tumors or low-grade (grade I and II) and malignant tumors or high-grade (grade III and IV) according to the World Health Organization (WHO) [1]. Some benign brain tumors are Gliomas (low-grade Gliomas LGG), and most malignant brain tumors are Gliomas (high-grade Gliomas HGG).
Due to the considerable progress in medical image acquisition devices comprises different modalities and processes, including Magnetic Resonance Imaging (MRI), Computed Tomography (CT), Positron Emission Tomography (PET) [2], among others, the medical data is quite voluminous. With the provision of comprehensive information and the support of multimodal MRI brain images, doctors can perform quantitative analyses of brain tumors such as the diameter, volume, and maximum amount of brain lesions, which allows the development of a diagnosis and optimal treatment plan for patients.

This manual brain tumor diagnosis is often painstaking. It requires significant and tedious efforts on the medical expert that can be highly subjective, evaluations and prognoses can be slow [3]. This

focuses on the advanced deep learning algorithms that can play a pivotal role in supporting clinicians in detecting different forms of tumors. A commonly used deep learning method for image segmentation and classification is to train a Convolutional Neural Network (CNN).
In this work, we propose an accurate and fully automatic system for classifying brain tumors into two classes High-Grade Glioma (HGG) and Low-Grade Glioma (LGG) from volumetric 3D Magnetic Resonance Imaging (MRI). The trained three well-known architectures, VGG-16, ResNet-50, and Inception V3, on four converted datasets (T1, T1ce, T2, and FLAIR) to select the most informative modality which presents more specific features and information to distinguish between LG and HG gliomas, passing by image pre-processing and data augmentation. Furthermore, non-tumorous slices in both HGG and LGG classes can lead to false negatives in the predicted output results. Therefore these slices were removed from the HGG class of the selected dataset, and then the three models were trained on this pre-processed dataset. Finally, we have proposed an algorithm that classifies the whole volume using just one modality with the accurate model.
The remaining paper is as follows: section 2 provides a summary of the current state-of-the-art in automated brain tumor classification and segmentation, section 3 introduces the proposed method, section 4 reports and discusses experimental results performed using the BraTS 2019 database. The last section includes the conclusion of this work.

2. Related work

Nowadays, brain tumors are among the most dangerous, rapidly growing types of cancer and deadliest diseases. Specialists try to use different technics for detecting these tumors and localizing them (manually). Its performance depends on pathologists' experience, and this did not help so much due to long time consumption and human errors.
Researchers pay attention to deep learning and its great performance in image classification and segmentation; due to their self-learning and generalization ability using large amounts of data.
Over the last ten years, many researchers have focused on the segmentation and classification of tumors on MRI images of the brain, particularly with data availability through the Brain Tumor Segmentation (BraTS) Challenge. Since this database's appearance in 2012, many researchers have contributed to the segmentation and classification of the different versions of this database.

Among the most recent works, Gonbadi et al. [4] preprocessed two databases, IXI dataset (refers to normal brains) and BraTS 2017(refers to glioma brain tumors), with the aim of classifying Glioma Brain Tumors by extracting the brain from the skull using Brain Extraction Tool (BET). They use CNN model built by gathering several layers (Convolution, Max-pooling, Up-sampling, Dense) to extract high level and low-level features from input images and finally classify them to three categories: HGG, LGG or normal brain. In the end, they got a desirable accuracy of 99.18%.

In 2019, Linmin Pei et al. [5] suggested a method for brain tumor classification which composed of two parts: the first use a 3D deep neural network for brain tumor segmentation on the multimodal magnetic resonance images, and the second part use also a 3D deep neural network that is developed for tumor classification using tumor segmentation results. Their paper applied their model on a dataset of Computational Precision Medicine: Radiology-Pathology Challenge (CPM: Rad-Path) for Brain Tumor Classification 2019. They obtained a dice score of 0.749 and an F1score of 0.764 for the validation data, while 0.596 for the dice score and 0.603 for the F1score in the test phase.

In [6], the authors proposed for the tumor segmentation task a Fully Convolutional Neural Network (FCNN) with three-layer deep encoder-decoder architecture is used along with dense connection at the encoder part. They have performed pre-processing using Z score normalization on individual MR sequences and data augmentation by rotation, flip, elastic transformation, shear, shift, and zoom on MRI sequences. The network training on BraTS 2019 uses the focal loss function. Initially, the network trains on the whole tumor, and then its weights are transfer to substructure network

training. Radiomic features from the segmentation results, age, and statistical features are used to predict patients' overall survival using random forest regressors. They obtained a dice similarity of training dataset with focal loss implementation for whole tumor, tumor core, and enhancing tumor is 0.92, 0.90, and 0.79, respectively. The overall survival prediction method outperformed the other methods with 58.6% accuracy for the validation dataset on the leaderboard and the test set of BraTS 2019 with 57.9% accuracy.

In the work of Alqazzaz et al. [7], the authors proposed a fully convolutional neural network SegNet to segment the entire tumor volume and accurately segment the tumor into four sub-tumor parts. Their work has four main steps: a pre-processing step, in which N4ITK bias field correction is applied to all MRI modalities, a training step to fine-tune separately four pre-trained SegNet models with 3D data sets with Flair, T1, T1ce, and T2 modalities as input data, a post-processing step to extract four maximum feature maps from the SegNet models' score maps, for the last step these feature maps are combined with the pixel values of the original MRI models, and they are taken as the input to a dataset classifier to further classify each pixel. Experimental results demonstrate that this method has the potential to perform well on brain tumor segmentation. Evaluating on BraTS 2017, F-measure scores give 0.85, 0.81, and 0.79 for whole tumor, tumor core, and enhancing tumor, respectively.

In more recent work, Mzoughi et al. [8] proposed a pre-processing technique based on intensity normalization and adaptive contrast enhancement of MRI data, and they applied a Deep Multi-Scale 3D Convolutional Neural Network on Brats 2018 dataset to classify Gliomas brain tumors into two classes: HGG and LGG. The proposed method offers an overall accuracy of 96.49% using the validation dataset.

3. Methods

In a human's life routine, the brain functions work continued through billions of interconnected neurons. This is the power of the human brain and the reason to imitate its general idea of working by building a network of interconnected artificial neurons, to perform several tasks like data processing, object detection, speech recognition, language translation, and decision making.
Some of these neural networks are built with many parameters and layers (more than five layers), which means we are talking about deep learning (DL). DL is the best solution for dealing with a large volume of data because its networks are modeled on similar human brain networks.
Deep learning (DL) is a subfield of machine learning (ML), and artificial intelligence (AI) concerned with algorithms driven by the structure of the brain and mimic the way humans analyzing, collecting, and interpreting knowledge. It is one of the important data science elements, which makes processing data and creating patterns for use in decision making faster and easier [9] [10]. Its networks capable of learning with and without human supervision (learn from labeled and unlabeled data).
For supervised learning tasks, deep learning methods eliminate feature engineering by translating the data into compact, intermediate representations akin to principal components and derive layered structures that remove redundancy in representation. The best-known architectures in supervised learning are the Convolution Neural Network (CNN). This type of neural network is trained by using big data and owns the capability of extracting features from data via convolutions without manual extraction of features. It comprises several kinds of layers: an input layer, an output layer, and hidden layers. The hidden layers consist of convolutional layers, ReLU layers, pooling layers, and fully connected layers, as is presented in Figure 1. Convolution neural network is one of the most popular deep learning architectures used for the classification and recognition of image, text, and sound [11] [12].

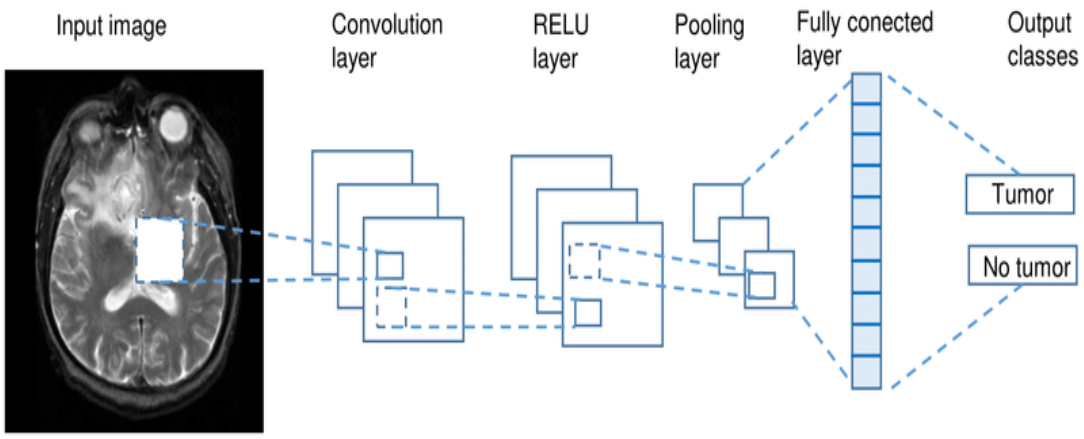

Figure 1. High-level general CNN architecture [11]

In this work, we have used three well-known and widely used architectures in the literature: VGGNet (VGG16), ResNet50, and InceptionV3.

3.1. VGGNet: This architecture was introduced by the Visual Geometry Group (Oxford University), VGG [13] is a Convolutional Neural Network architecture based on AlexNet. There are two architectures of VGG: VGG16 & VGG19. The architecture contains:

- Input: VGG used RGB image in a 224x224 pixel.
- Convolutional Layers: In VGG, the convolutional layers use a very small receptive field 3x3. There are also 1x1 convolution filters, which can be seen as a linear transformation of the input channels, followed by a ReLU layer. The convolution stride is fixed to 1 pixel.
- Max Pooling: is performed over a 2×2 pixel window.
- Fully-Connected Layers. VGG contained three fully- connected layers.
- Hidden Layers: All hidden layers are equipped with the non-linearity layer (ReLU). Not all networks contain Local Response Normalisation (LRN) due to their memory and time consuming and does not improve the performance.

VGG16 contained 16 layers (13 convolutional layers + 3 fully connected layers); it is very used due to its uniform Architecture. In the community of extracting features from images, VGG16 is one of the most preferred networks.

3.٢. ResNet: Deeper networks can provide more complex features, increasing the robustness and performance of the model. However, adding more layers to the network does not work by simply stacking layers together. Deeper neural networks are difficult to train because of vanishing and exploding gradient types of problems. ResNet [14], one of the common architectures of CNN, allowed us to train extremely deep neural networks.

Residual Networks 'ResNets' are nearly similar to networks with layers of convolution, pooling, activation, and fully-connected layers. The basic building block for ResNets is the convolutional and identity blocks, which connect the output of one layer with the input of an earlier layer (skip connection). There are many variants of the ResNet architecture depending on the number of layers, such as ResNet-50, ResNet-101, ResNet-110, and ResNet-152.

The architecture of ResNet-50 consists of 5 stages. Every ResNet architecture carries out the initial convolution and max-pooling using 7×7 and 3×3 kernel sizes, respectively. Each convolution block has three convolution layers, and each identity block also has three convolution layers. The network also has an Average Pooling and a fully connected layer with 1000 neurons (ImageNet class output).

3.3. Inception network: It is a convolutional neural network (CNN) characterized -in addition to its common layers- by its unique module, "Inception module", which was designed to solve the problem of computational expense and overfitting, among other issues. In general Inception network is one of the possible solutions for computer vision problems. The popular versions of inception networks are as follows:

- Inception v1 or GoogLeNet
- Inception v2 and Inception v3.
- Inception v4 and Inception-ResNet.

Inception module:

The inception module combines convolution layers with different filter sizes (5X5, 3X3, 1X1) and max pooling. It has a bottleneck layer (1X1 convolutions) used for dimensionality reduction, then concatenate all of their output into a single output vector to form the input of the next layer. The object from the convolutions of different sizes is to capture details at varied scales [15].

Inception v3:

Inception V3 [16] is the 3rd version of inception architectures characterized by additional factorization ideas.

Inception V3 is a widely used model for image recognition; this model comprises multiple blocks, including convolutions, average pooling, max pooling, concatenations, dropouts, and fully connected layers and using the Batch norm to activate inputs also the Softmax to compute the Loss.

In this study, we have performed a transfer learning on the VGG16, ResNet-50, and InceptionV3 by reusing the weights from the pre-trained models on the ImageNet dataset.

4. Results and Discussions

In this study, we are interested in the classification of brain tumors into two classes (LGG and HGG). We will first test three well-known architectures on the BraTS dataset to perform this task, then perform a dataset pre-processing, after that image classification, and finally a full volume classification.

4.1. Used dataset:

BraTS utilizes multi-institutional pre-operative MRI scans and primarily focuses on the segmentation (Task 1) of intrinsically heterogeneous (in appearance, shape, and histology) brain tumors, namely gliomas. Furthermore, to pinpoint this segmentation task's clinical relevance, BraTS also focuses on predicting overall patient survival (Task 2) and intends to classify volumes in HGG and LGG classes (Task 3). All BraTS multimodal scans (volumes from 335 patients: 259 HGG and 76 LGG volumes) are available as NIfTI files (.nii.gz) and were acquired with different clinical protocols and various scanners from multiple institutions.

BraTS contains four modalities: a) native (T1) and b) post-contrast T1-weighted (T1Gd), c) T2-weighted (T2), and d) T2 Fluid Attenuated Inversion Recovery (T2- FLAIR) volumes.

All the imaging datasets have been segmented manually,

One to four raters, following the same annotation protocol, and their annotations were approved by experienced neuro- radiologists [17].To train and test our classification model, we have selected a subset from the BraTS dataset and divided it into four databases, one for each modality. Each modality from the previous four databases contains 155 slices for one patient; in this paper, we will work with these slices as PNG images. The used databases provided as a set of slices contain 2015 High-Grade Glioma (HGG) and 2015 Low-Grade Glioma (LGG) images from the T1, T1ce, T2, and FLAIR modalities, respectively. The examples of High and Low-Grade Glioma obtained by T1, T1ce, T2, and FLAIR modalities are shown in Figures 2 and 3.

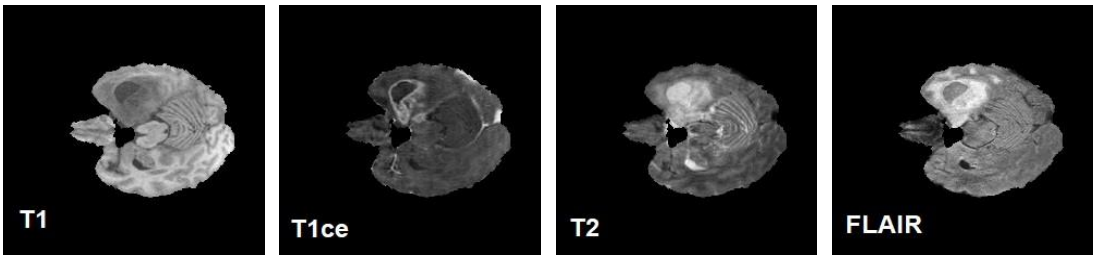

Figure 2. HGG images

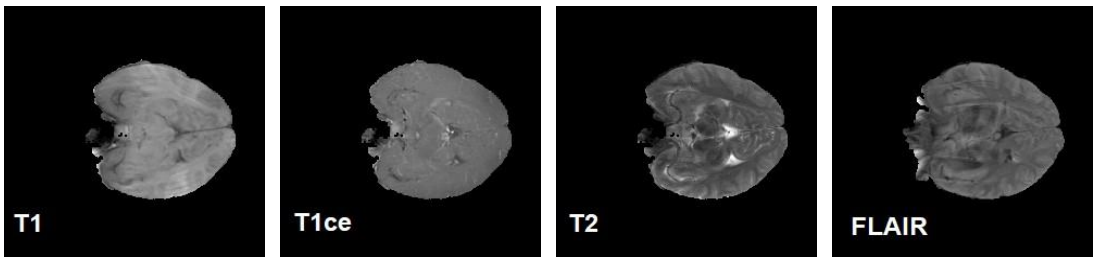

Figure 3. LGG images

4.2. Modality selection

As mentioned before, the BraTS database contains four modalities (T1, T2, T1ce, and FLAIR). This study aims to select the best modality that contains the best information for the classification of brain cancer. Such a study allows us, in the future, to acquire only the most informative modality and thus reduce the cost of MRI.

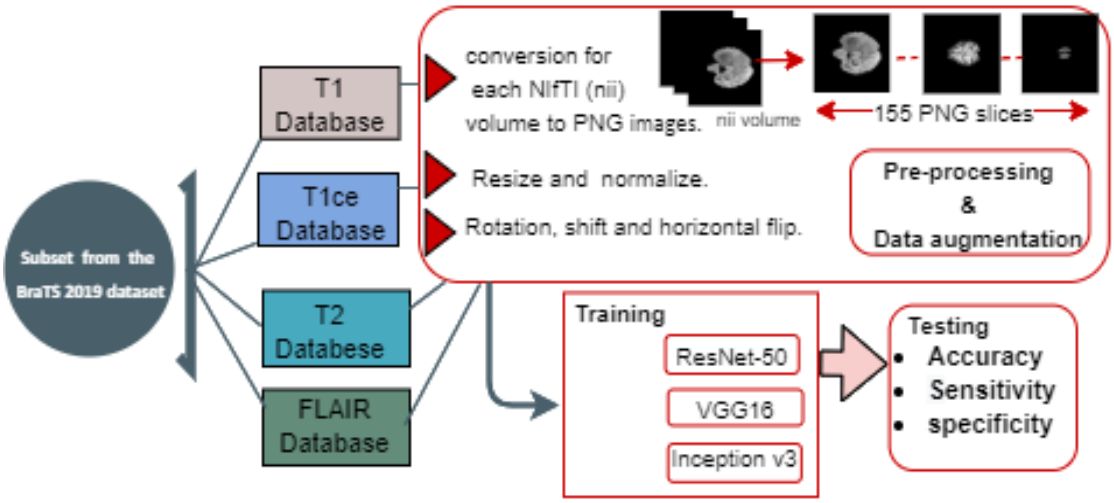

Figure 4. Block diagram: the process of the selection of the database which allows the models to train well.

As shown in Figure 4, we have converted each NIfTI (nii) volume to PNG images; thus, each volume gives us 155 PNG images. We have normalized and readjusted all images' sizes to use them with the deep learning models (224*224 for VGG16 and ResNet50 and 299*299 for InceptionV3).To augment the datasets, we transformed each image by rotation, shift, and horizontal flip.

Brain tumor classification was performed using a set of CNN models developed using Keras and Tensorflow on a local machine with a 4820k i7 processor, 56 GB RAM, 8 GB GTX1070 GPU, and Windows 10 operating system.

The classification was achieved using transfer learning on three pre-trained models on the ImageNet database: VGG16, ResNet50, and Inception v3; and BraTS 2019 database divided into four databases for each modality. All the models were trained for 50 epochs using a batch size equal to 16 with an SGD optimizer to minimize the loss function.

Firstly, we applied the chosen models on the first version of our databases (4 datasets without pre-processing) to find which modality helped them train well. The results of this training are shown in Table 1, where Equations (1), (2), and (3) show how to compute specificity, sensitivity, and accuracy, respectively:

$$\text{Specificity} = (TN) /(TN + FP) = \text{Probability of being test negative when disease absent,} \quad (1)$$

$$\text{Sensitivity} = (TP) /(TP + FN) = \text{Probability of being test positive when disease present,} \quad (2)$$

$$\text{Accuracy} = (TN + TP) /(TP + FN + TN + FP), \quad (3)$$

With:

- True Positive (TP) is the number of positive predicted cases and they are actually positive.
- True Negative (TN) is the number of negative predicted cases and they are also actually negative.
- False Negative (FN) is the number of negative predicted cases while they are actually positive.
- False Positive (FP) is the number of positive predicted cases while they are actually negative.

Table 1. The calculated performances of the three models applied on four databases.

Dataset	Model	Accuracy	Sensitivity	Specificity
T1CE	Resnet50	0.9413	0.8894	0.9925
	VGG16	0.9438	0.8945	0.9925
	InceptionV3	0.9488	0.8995	**0.9975**
Flair	Resnet50	0.9437	0.8944	0.9925
	VGG16	0.9474	0.8969	**0.9975**
	InceptionV3	0.9487	0.8994	**0.9975**
T1	Resnet50	**0.9513**	**0.907**	0.9487
	VGG16	0.9413	0.8894	0.9925
	InceptionV3	0.95	0.9045	0.995
T2	Resnet50	0.9475	0.8969	**0.9975**
	VGG16	0.9424	0.8944	0.99
	InceptionV3	0.9463	0.8969	0.995

Table 1 summarizes the results obtained by three models learned on four databases (T1, T2, Flair, and T1CE without pre-processing). We noticed a difference in the performance of models in terms of accuracy, sensitivity, and specificity. In general, diagnostic support systems depend on metrics to measure how well they predict the outcomes; one of the important metrics is sensitivity.

The higher value of sensitivity means a lower value of false negative. In other words, patients who are unhealthy and got predicted as healthy. For that in Brain tumors classification, this metric is highly important and puts the focus on it. Based on sensitivity values, we can compare the obtained results in training on each dataset to find the one that will give the best generalization also the best performance with these models, so this database is the T1 database.

One of the major challenges in the converted volumes to 155 PNG images is non-tumorous slices in both HGG and LGG classes. These slices can lead to a wrong classification in the predicted output results.

Secondly, we initiated training with the preceding models on the T1 pre-processed database.

4.3. Brain tumor image classification

We have noticed that the volume of HGG contains some black slices, which are also found in LGG volumes. To avoid misclassifying these images, since they do not contain any information, we have removed them from the HGG database. Such an action will allow us to consider all black slices as

LGG and reduce the error rate. The obtained results with this pre-processing step are shown in Table2. The same models (VGG16, ResNet50, and Inception V3) were applied on the T1 pre-processed dataset (see Figure 5) to select the best model for this pre-processed modality.

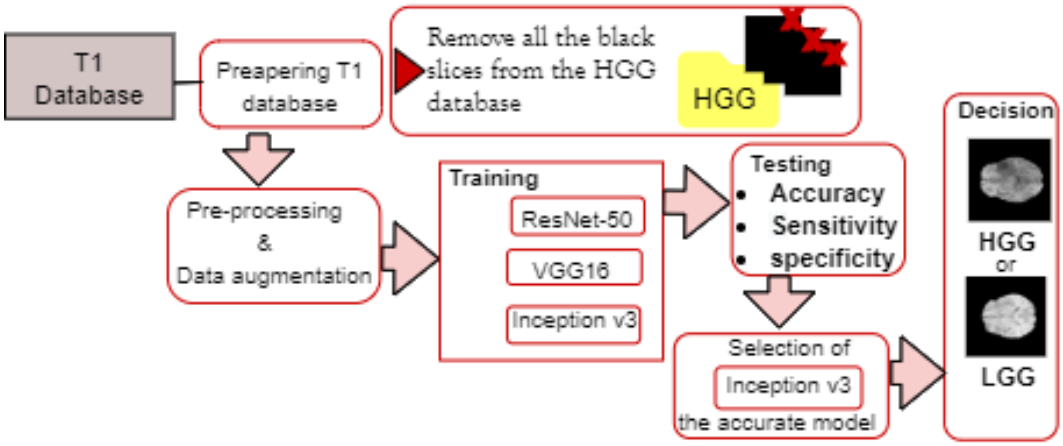

Figure 5. Block diagram: the process of the selection of the best model for the T1 pre-processed database.

Table 2. The obtained results of performances of training three models on pre-processed T1 dataset.

Dataset	Model	Accuracy	Sensitivity	Specificity
T1 pre-processed	Resnet50	0.9971	0.9876	0.9937
	VGG16	0.9954	0.9805	1
	InceptionV3	**0.9975**	**0.9894**	**1**

According to the found results and the ranking of models based on their performances in Table 2, Inception v3 exceeds the others regarding the highest values of precision, sensitivity, and specificity. This overall improvement of the results can be explained by the fact that removing the black slices has allowed the model to focus on the images that contain relevant information and remove the classification error for these black images since they were previously included in both classes.
The final objective of this work is to classify the volumes in HGG and LGG; for this, we proposed a solution to realize this task.

4.4. Volume classification

Algorithm 1 presents the process of classifying a total volume for one patient that used only one modality (T1 with the conversion from nii volume to 155 slices PNG images) from the whole volume. The Inception V3 model classifies each image, and at the same time, a counter is increasing if the class was HGG; if it is an LGG image, the counter will not be increased. The counter will be tested if at least one image is classified as HGG class, which means the patient has an HGG tumor; if not (counter =0), that means the patient has an LGG tumor.
We have used this algorithm to validate our results on ten volumes (5 HGG and 5 LGG). We obtained a classification rate of 100% (all ten volumes were well classified) with an average certainty rate close to 95%. These results confirm that physicians can trust our application for potential use in brain cancer diagnosis.
We also proposed in this work a web application to deploy our model and facilitate its use by physicians.

Algorithm 1: Brain Tumor classification

```
Data: Brain MRI volume (T1 modality) MRI
Result: Decision (HGG or LGG) D
initialization: i=0;
IMG = decomposition(MRI);
for each IMG do
    cl = classify(IMG);
    if cl == 'HGG' then
        i++;
    end
end
if i >0 then
    D = 'HGG';
else
    D = 'LGG';
end
```

In this application (see Figure 6), the physician, after authentication, loads the T1 volume of the MRI. This volume will be decomposed into 155 PNG images. These images will be classified using our Inception V3 model.

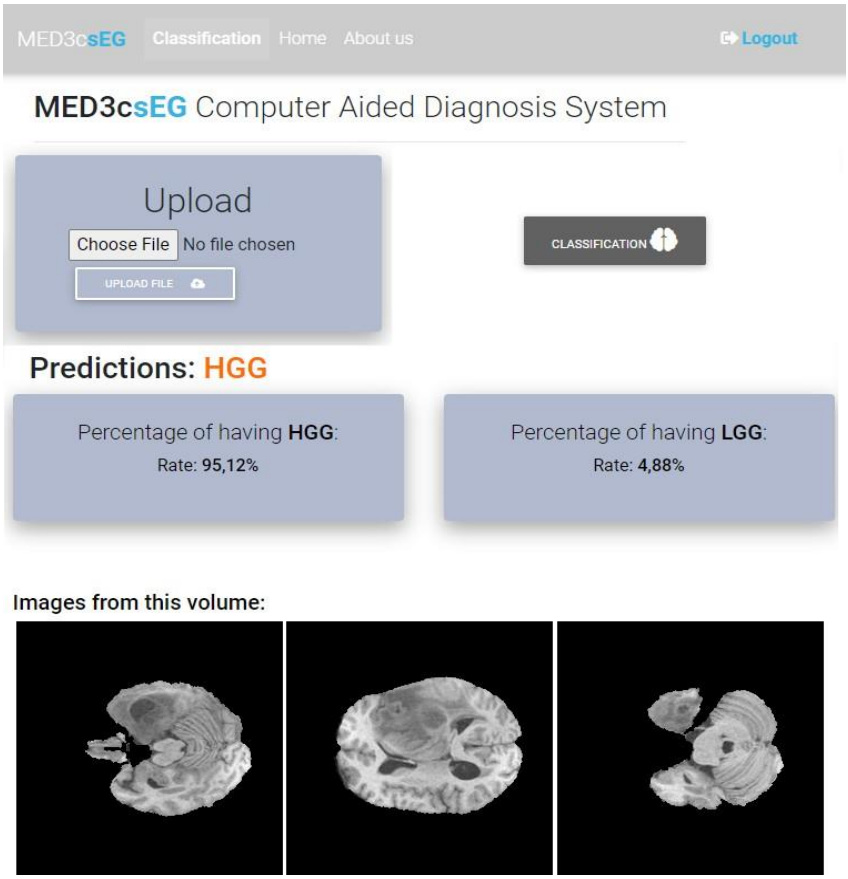

Figure 6. Our proposed web application

Our web application will help doctors to make decisions. Indeed, at the end of the classification, a label will be affected to the 3D volume and displayed with a degree of precision and a sample of the images that contributed to this decision.

5. Conclusions

Brain tumors affect the human's life improperly because of the abnormal growth of cells inside the brain. It may disturb brain function and be dangerous and life-threatening. Brain tumors are grouped into two categories benign tumors and malignant tumors. One of the different types of medical imaging technologies based on a non-invasive approach is MRI that offers greater contrast images - especially of the brain- that provides different information about the shape or function of organs in the patient's body. Doctors base their decisions on this information, but unfortunately, this kind of data is extremely difficult to exploit quantitatively and objectively. In this work, our proposed approach aims to help the doctor by classifying MRI volumes into two classes HGG and LGG. First, we have performed a decomposition of each modality (T1, T2, T1ce, and Flair) of the MRI volumes to 155 PNG images. These images were used to train and test three well-known CNN architectures in the state-of-the-art. This experiment aimed to choose the best modality in the classification of brain tumors. The results show that the T1 gives the best performances. We have noticed that the LGG and HGG volumes contain black slices, leading to misclassification. To solve this problem, we have proposed to delete these images from the HGG dataset. This pre-processing step allowed the model to increase the accuracy rate using the Inception V3, and it obtains 0.9975, 0.9894, and 1 for the accuracy, sensitivity, and specificity, respectively. Finally, we have proposed an algorithm that classifies the whole volume. Based on the obtained results, we can conclude that such a system will be of great use to radiologists in helping to diagnose brain cancer.

Acknowledgments: The authors would like to thank the Directorate-General of Scientific Research and Technological Development (Direction Générale de la Recherche Scientifique et du Développement Technologique, DGRSDT, URL: www.dgrsdt.dz, Algeria) for the financial assistance towards this research.

References

1. D. N. Louis, A. Perry, G. Reifenberger, A. Von Deimling, D. Figarella- Branger, W. K. Cavenee, H. Ohgaki, O. D. Wiestler, P. Kleihues, and D. W. Ellison, "The 2016 world health organization classification of tumors of the central nervous system: a summary," Acta neuropathologica, vol. 131, no. 6, pp. 803–820, 2016.
2. M. D. Guimara˜es, J. Noschang, S. R. Teixeira, M. K. Santos, H. M. Lederman, V. Tostes, V. Kundra, A. D. Oliveira, B. Hochhegger, and E. Marchiori, "Whole-body mri in pediatric patients with cancer," Cancer Imaging, vol. 17, no. 1, pp. 1–12, 2017.
3. D. Shen, G. Wu, and H.-I. Suk, "Deep learning in medical image analysis," Annual review of biomedical engineering, vol. 19, pp. 221– 248, 2017.
4. F. B. Gonbadi and H. Khotanlou, "Glioma brain tumors diagnosis and classification in MRI images based on convolutional neural networks," in 2019 9th International Conference on Computer and Knowledge Engineering (ICCKE), 2019, pp. 1–5.
5. L. Pei, L. Vidyaratne, W.-W. Hsu, M. M. Rahman, and K. M. Iftekharud- din, "Brain tumor classification using 3d convolutional neural network," in International MICCAI Brain lesion Workshop. Springer, 2019, pp. 335–342.
6. R. R. Agravat and M. S. Raval, "Brain tumor segmentation and survival prediction," in International MICCAI Brainlesion Workshop. Springer, 2019, pp. 338–348.
7. S. Alqazzaz, X. Sun, X. Yang, and L. Nokes, "Automated brain tumor segmentation on multi-modal mr image using segnet," Computational Visual Media, vol. 5, no. 2, pp. 209–219, 2019.
8. H. Mzoughi, I. Njeh, A. Wali, M. B. Slima, A. Ben Hamida, C. Mhiri, and K. B. Mahfoudhe, "Deep multi-scale 3d convolutional neural network (CNN) for MRI gliomas brain tumor classification," Journal of Digital Imaging, 2020.
9. V. Kumar and M. L., "Deep learning as a frontier of machine learning: A review," International Journal of Computer Applications, vol. 182, pp. 22–30, 07 2018.

10. A. Muniasamy and A. Alasiry, "Deep learning: The impact on future elearning," International Journal of Emerging Technologies in Learning (iJET), vol. 15, p. 188, 01 2020.
11. J. Ker, L. Wang, J. Rao, and T. Lim, "Deep learning applications in medical image analysis," Ieee Access, vol. 6, pp. 9375–9389, 2017.
12. Y. LeCun, Y. Bengio, and G. Hinton, "Deep learning," nature, vol. 521, no. 7553, pp. 436–444, 2015.
13. K. Simonyan and A. Zisserman, "Very deep convolutional networks for large-scale image recognition," arXiv preprint arXiv:1409.1556, 2014.
14. K. He, X. Zhang, S. Ren, and J. Sun, "Deep residual learning for image recognition," in Proceedings of the IEEE conference on computer vision and pattern recognition, 2016, pp. 770–778.
15. X.-F. Xu, L. Zhang, C.-D. Duan, and Y. Lu, "Research on inception module incorporated siamese convolutional neural networks to realize face recognition," IEEE Access, vol. 8, pp. 12 168–12 178, 2019.
16. C. Szegedy, W. Liu, Y. Jia, P. Sermanet, S. Reed, D. Anguelov, D. Erhan, V. Vanhoucke, and A. Rabinovich, "Going deeper with convolutions," in Proceedings of the IEEE conference on computer vision and pattern recognition, 2015, pp. 1–9.
17. P. Spyridon Bakas, "Multimodal brain tumor seg- mentation challenge 2020: Data." [Online]. Available: https://www.med.upenn.edu/cbica/brats2020/data.html